

P. 23

FINAL REPORT

CONTRACT NO: NAS5-30883

JULY 1992

SUBMITTED TO:

**NASA GODDARD SPACE FLIGHT CENTER
ENGINEERING PROCUREMENT OFFICE
GREENBELT ROAD
GREENBELT, MD 20771**

SUBMITTED BY:

**OPTRA, INC.
66 CHERRY HILL DRIVE
BEVERLY, MA 01915**

PROGRAM MANAGER: ANDREW LINTZ

(NASA-CR-191328) [MEASURING
ELECTRICALLY CHARGED PARTICLE
FLUXES IN SPACE USING A FIBER OPTIC
LOOP SENSOR] Final Report (OPTRA)
23 p

N94-23829

Unclas

G3/74 0204534

OPTRA

TABLE OF CONTENTS

| | <u>PAGE</u> |
|-----------------------------|-------------|
| 1. INTRODUCTION..... | 1 |
| 2. THEORY OF OPERATION..... | 1 |
| 3. SENSOR DESIGN..... | 2 |
| 4. SYSTEM PERFORMANCE..... | 11 |
| 5. CONCLUSION..... | 19 |

LIST OF FIGURES

| | | |
|-----------|---------------------------------------|----|
| FIGURE 1 | SOURCE MODULE..... | 2 |
| FIGURE 2 | HIGH BIREFRINGENCE OPTICAL FIBER..... | 3 |
| FIGURE 3 | LOW BIREFRINGENCE OPTICAL FIBER..... | 4 |
| FIGURE 4 | FIBER OPTIC LOOP II..... | 6 |
| FIGURE 5 | FIBER OPTIC LOOP II..... | 7 |
| FIGURE 6 | RECEIVER OPTICS..... | 7 |
| FIGURE 7 | SIGNAL PROCESSOR BLOCK DIAGRAM..... | 9 |
| FIGURE 8 | SYSTEM PERFORMANCE..... | 12 |
| FIGURE 9 | PHASE SIGNAL..... | 13 |
| FIGURE 10 | FREQUENCY RESPONSE..... | 14 |
| FIGURE 11 | SENSOR LINEARITY..... | 15 |
| FIGURE 12 | FREQUENCY RESPONSE..... | 16 |
| FIGURE 13 | SYSTEM DC DRIFT..... | 17 |
| FIGURE 14 | DC DRIFT (NO LOOP)..... | 17 |
| FIGURE 15 | OPTICAL PATH DIFFERENCE..... | 18 |

LIST OF APPENDICES

| | |
|-----------------|-------|
| APPENDIX A..... | 20-21 |
|-----------------|-------|

1. INTRODUCTION

The purpose of this program was to demonstrate the potential of a fiber optic loop sensor for the measurement of electrically charged particle fluxes in space. The key elements of the sensor are a multiple turn loop of low birefringence, single mode fiber, with a laser diode light source, and a low noise optical receiver. The optical receiver is designed to be shot noise limited, with this being the limiting sensitivity factor for the sensor. The sensing element is the fiber optic loop. Under a magnetic field from an electric current flowing along the axis of the loop, there is a non-vanishing line integral along the fiber optic loop. This causes a net birefringence producing two states of polarization whose phase difference is correlated to magnetic field strength and thus, current in the optical receiver electronic processing.

The objectives in this program were to develop a prototype laser diode powered fiber optic sensor. The performance specification of a minimum detectable current density of $1 \mu\text{amp}/\text{m}^2\text{-}/\text{Hz}$, should be at the shot noise limit of the detection electronics.

OPTRA has successfully built and tested a 3.2 meter diameter loop with 137 turns of low birefringence optical fiber, and achieved a minimum detectable current density of $5.4 \times 10^{-5} \text{ amps}/\sqrt{\text{Hz}}$. If laboratory space considerations were not an issue, with the length of optical fiber available to us, we would have achieved a minimum detectable current density of $4 \times 10^{-7} \text{ amps}/\sqrt{\text{Hz}}$.

2. THEORY OF OPERATION

The overall program objective is the development of a space deployable sensor for measuring weak fluxes of charged particles in outer space. When an electric current passes through an optical fiber loop, the magneto-optic effect in the optical fiber produces a circular birefringence which can be expressed as a phase difference between right and left hand circularly polarized components transmitted through the fiber. This phase difference, ϕ , can be expressed as:

$$\phi = 2VNI$$

where ϕ is measured in radians, V is the Verdet constant of the optical fiber (fused silica), N is the number of turns of optical fiber making up the loop, and I is the electric current passing through the loop. If the current is due to a current density, J (amp/m^2), and an optical fiber of length L is formed into a loop diameter, D ($N = L/\pi D$), then:

$$\phi = VJDL/2$$

Thus the maximum responsivity to J for a given length of optical fiber is obtained by maximizing the diameter of the loop.

The combination of fiber loop and laser source produces an interferometric phase difference which is proportional to the current density inside the loop. The detection system generates three signals of different phases and interprets them in real time to generate a wrapped signal proportional to the input phase, modulo 2π . Then the phase unwrapping electronics generates a digital signal which replicates the input phase as a function of time.

To measure the small current densities discussed in this program, the sensitivity will be limited by the electronic noise in the signal processing system. Therefore it is necessary for the electronic detection system to be shot noise limited.

3. SENSOR DESIGN

The fiber optic loop sensor consists mainly of four integrated parts, the light source, the fiber optic loop, the receiver optics and the signal processing system.

The source module, shown in Figure 1 consists of a Sharp LT015, 40 mW, temperature stabilized, optically isolated laser diode with a high birefringence (HiBi) single mode optical fiber pigtail. This module package was purchased from Seastar Optics, British Columbia, Canada.

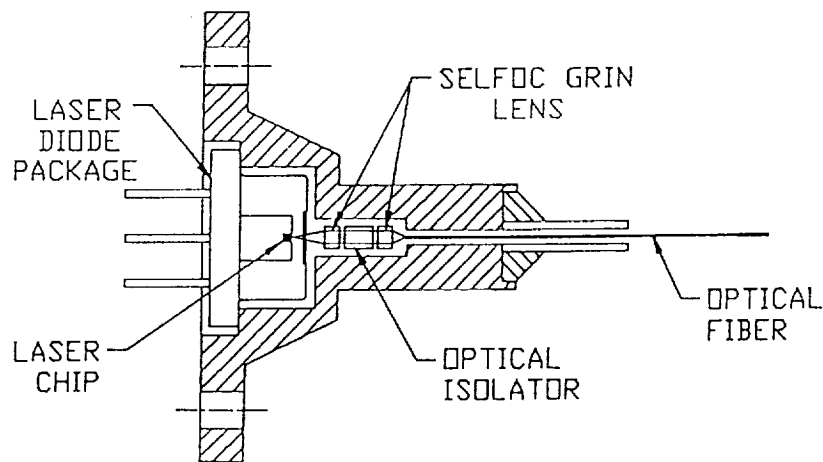


Figure 1 Source Module

Laser light is collimated through the use of a gradient index lens. A Faraday optical isolator provides approximately 50 dB of optical isolation, preventing the optical feedback caused by wavelength and amplitude instability observed in the Phase I program. A second gradient index lens couples the collimated light to the HiBi fiber. HiBi optical fiber, see Figure 2, was used to maintain the linear polarization from the laser source. This type of fiber is fabricated so that the modal birefringence is maximized. This is done by maximizing the geometrical portion of the birefringence through the use of a Bow-Tie core shape instead of a circular core shape. In addition to good polarization control, it also minimizes bend and temperature induced optical loss by increasing the core refractive index above that used in telecommunication fibers. It also acts as a polarizer, increasing the extinction ratio yielded by the laser itself, and as a spatial filter, producing a high quality beam.

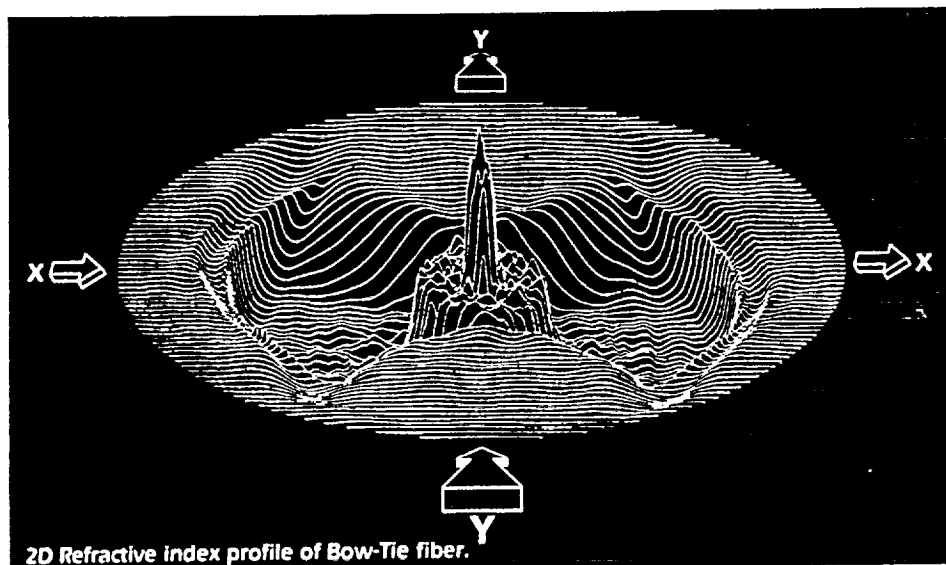


Figure 2 High Birefringence Optical Fiber

The optical fiber loop is constructed of York Low Birefringence (LoBi), $5/125\mu\text{m}$, single mode optical fiber. It consists of 1400 meters of fiber wound into a 3.2 meter diameter loop of 137 turns. Each turn has one 360° twist placed in it during winding. York LoBi fiber, see Figure 3, was used due to its negligible intrinsic birefringence - linear or circular. As this sensor operates via the Faraday effect, namely that a magnetic

field will rotate the plane of polarization of inputted linearly polarized light, low birefringence fiber is essential to allow the rotation of the polarized light due to external fields. The fiber is manufactured using a preform spinning technique developed at South Hampton University, England. As shown in the refractive index profile, the outer cladding is pure silica ($n = 1.457$) and the core index is higher to give a numerical aperture of 0.11 to 0.15. Between the cladding and the core is a deposited inner cladding. This cladding has an index very close to that of silica.

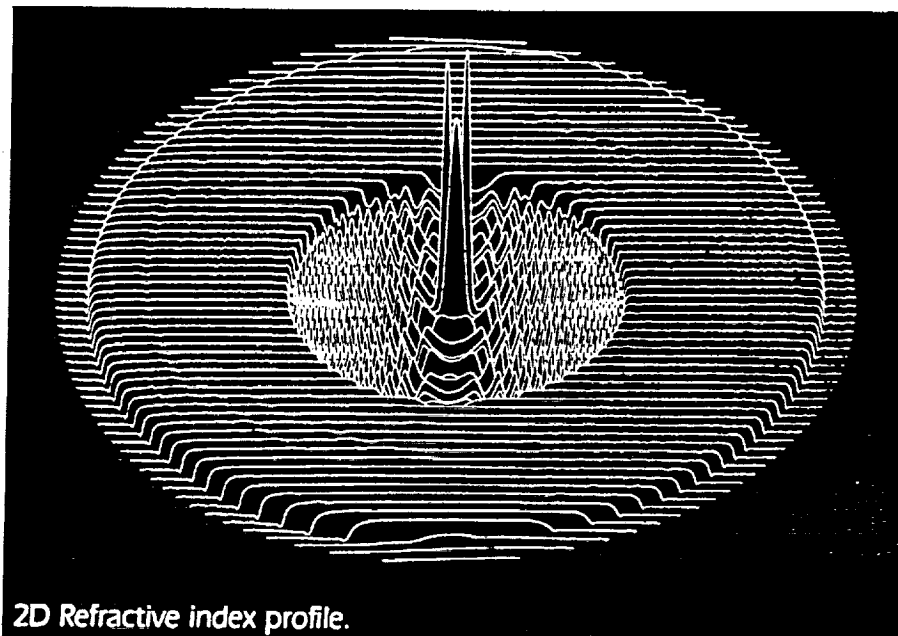


Figure 3 Low Birefringence Optical Fiber

The phase difference, Φ , initiated by the magnetic field passing through the loop, is expressed as:

$$\Phi = VJDL/2$$

where V is the Verdet constant of the fiber, J is the current density in amps/m^2 , and L is the optic fiber total length. The maximum responsivity is obtained by maximizing the diameter of the loop. The diameter of 3.2 meters was the largest available, given our working area. As we had 1400 meters available, we used all of it in 137 turns.

Although LoBi fiber has no polarization maintaining properties, by bending it into a loop, there is an induced polarization maintaining axis. The light that exits the source module via the HiBi fiber has a very well defined linear polarization axis with an extinction ratio of better than 350:1. The source and loop are joined by an FC type connector. The linear polarization direction was not aligned with respect to the keying of the connector. Therefore, when the loop and source are connected, the linear polarization is not aligned with the bend induced polarization maintaining axis of the loop. By twisting the FC connector (actually localized twisting of the input end of LoBi fiber), an effective linear polarization rotation is achieved. Essentially for every 12° of induced mechanical twist, 1° of linear polarization rotation is achieved.

Because the fiber is bent into a loop, the bend radius produces a bend induced birefringence. This can produce non-linearities in data. The bend birefringence, δ , is characterized by:

$$\delta = (0.25Kn^3L[\rho_{11} - \rho_{12}] [1 + \nu_p]\rho^2/R^2$$

where $K = 2\pi/\lambda = 2\pi/830 \text{ nm} = 7.57 \times 10^6 \text{ m}^{-1}$

$n = \text{fiber index} = 1.46$

$\rho_{11} - \rho_{12} = 0.12 - 0.27 = -0.15 = \text{component of strain optical tensor}$

$\nu_p = \text{Poisson's ration} = 1.16$

$\rho = \text{radius of fiber} = 63 \mu\text{m}$

$R = \text{radius of loop} = 5.25 \text{ m}$

$L = \text{length of fiber} = 1400 \text{ meters}$

Thus for our design, $\delta = -0.21$ radians. The bend birefringence can cause non-linearities and reduced Faraday effect rotation. These negative effects of bend birefringence can be overcome by inserting a known amount of twist into the loop, also known as the twist birefringence. As shown in Figures 4 and 5, the sensitivity versus current graphs show two plots overlaid. The ideal phase is the phase value, in radians, that you would expect using just the Faraday effect equation - no bend or twist birefringence. The plots showing twist values always have the calculated value of bend birefringence, $\delta = -0.21$ radians. Figures 4 and 5 show as you increase the twist amount effectively from zero total to one twist/turn, the bend birefringence is overcome, yielding an expected sensitivity close the ideal phase.

As the linearly polarized light enters the LoBi fiber it is decomposed into left and right hand circularly polarized components. The magnetic field associated with a current through the loop causes a refractive index difference, within the fiber, for the left and right circular components. This, in turn, produces an optical path difference between the two components. As shown in Figure 6, the light leaving the fiber is collimated

FIBER OPTIC LOOP II

Sensitivity vs. Current

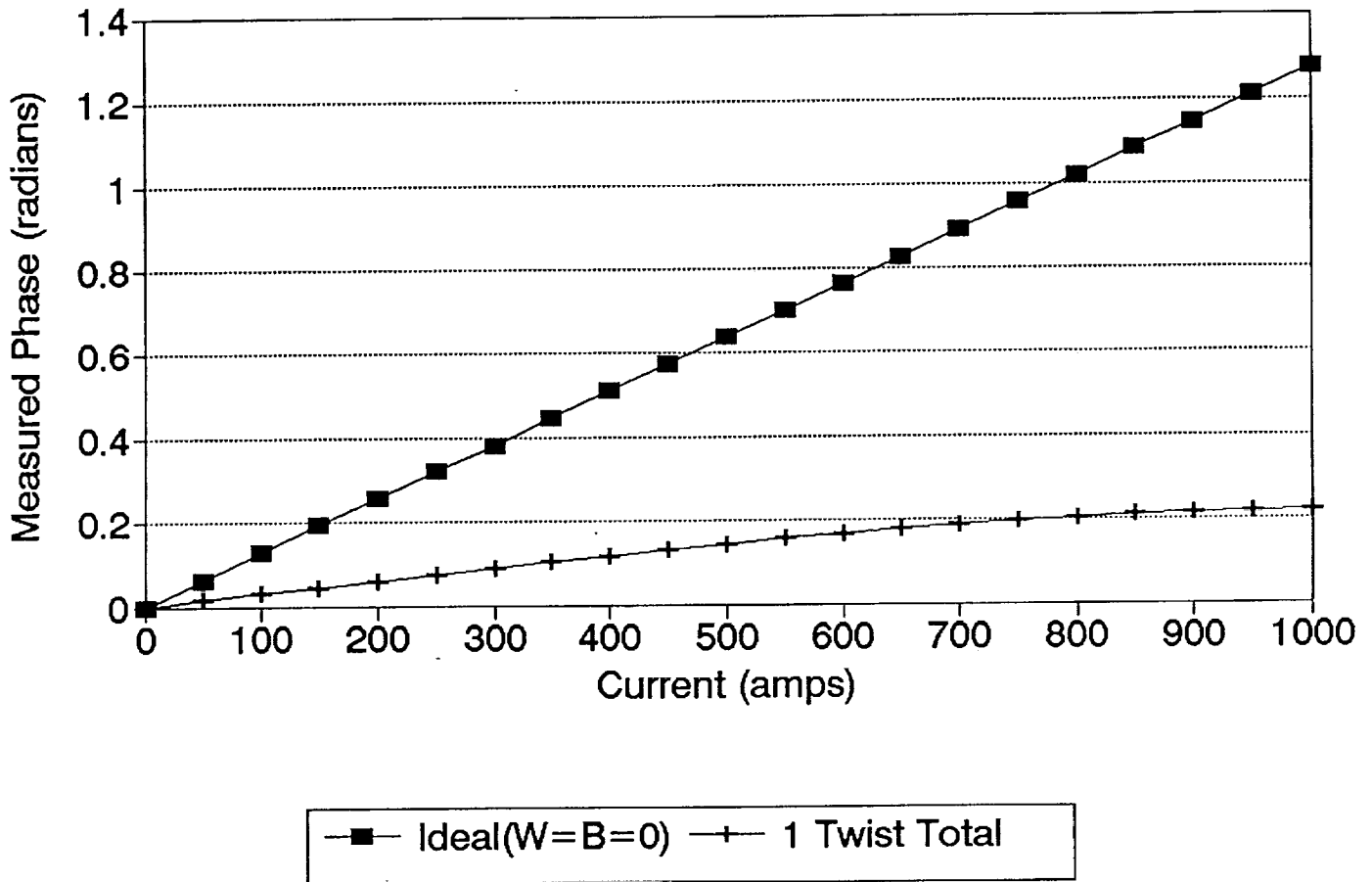


Figure 4

FIBER OPTIC LOOP II

Sensitivity vs. Current

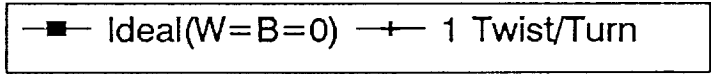
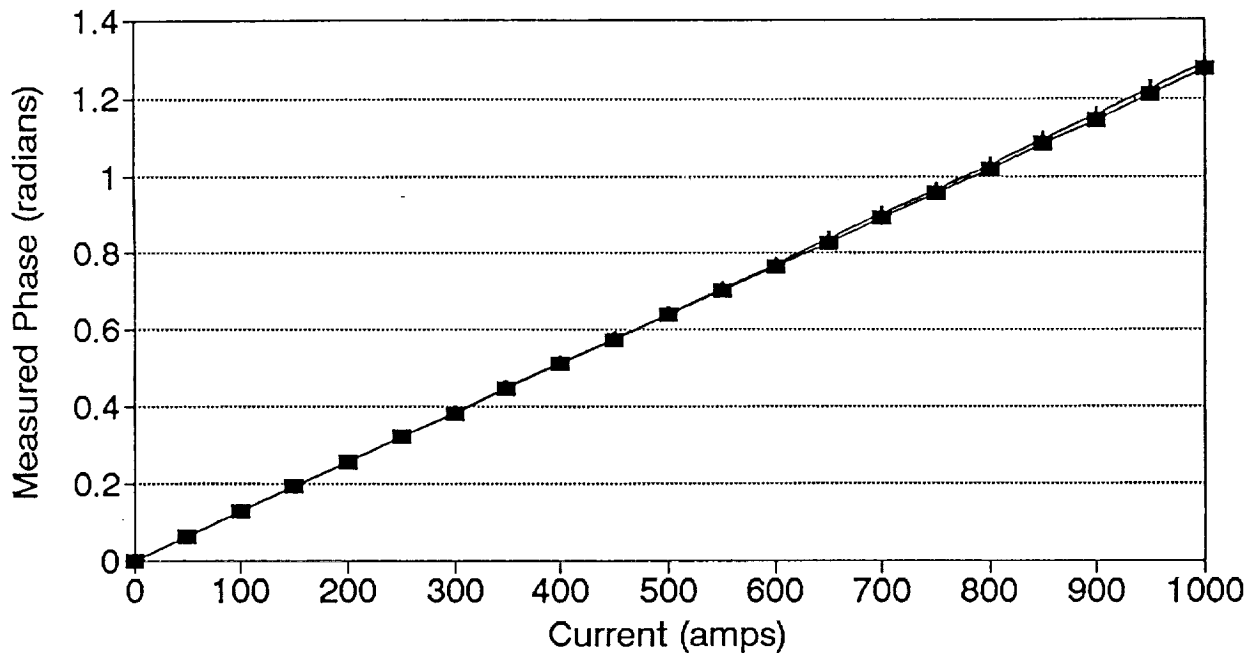


Figure 5

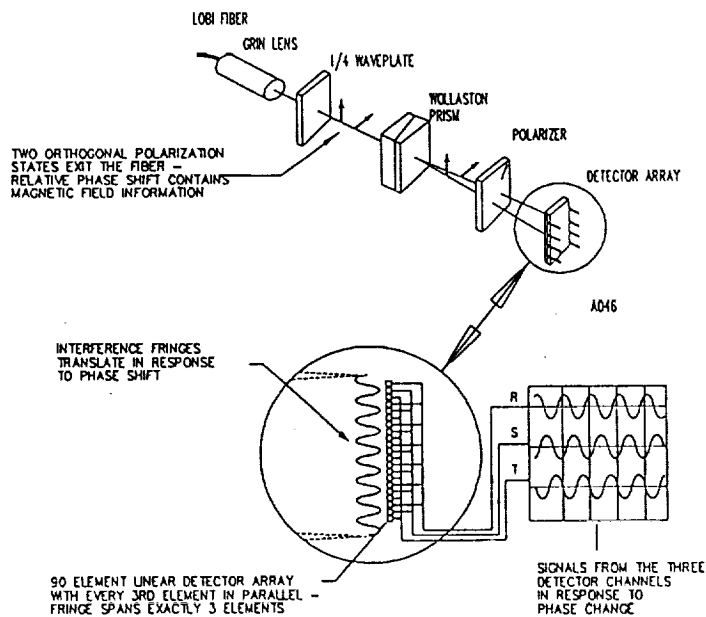


Figure 6 Receiver Optics

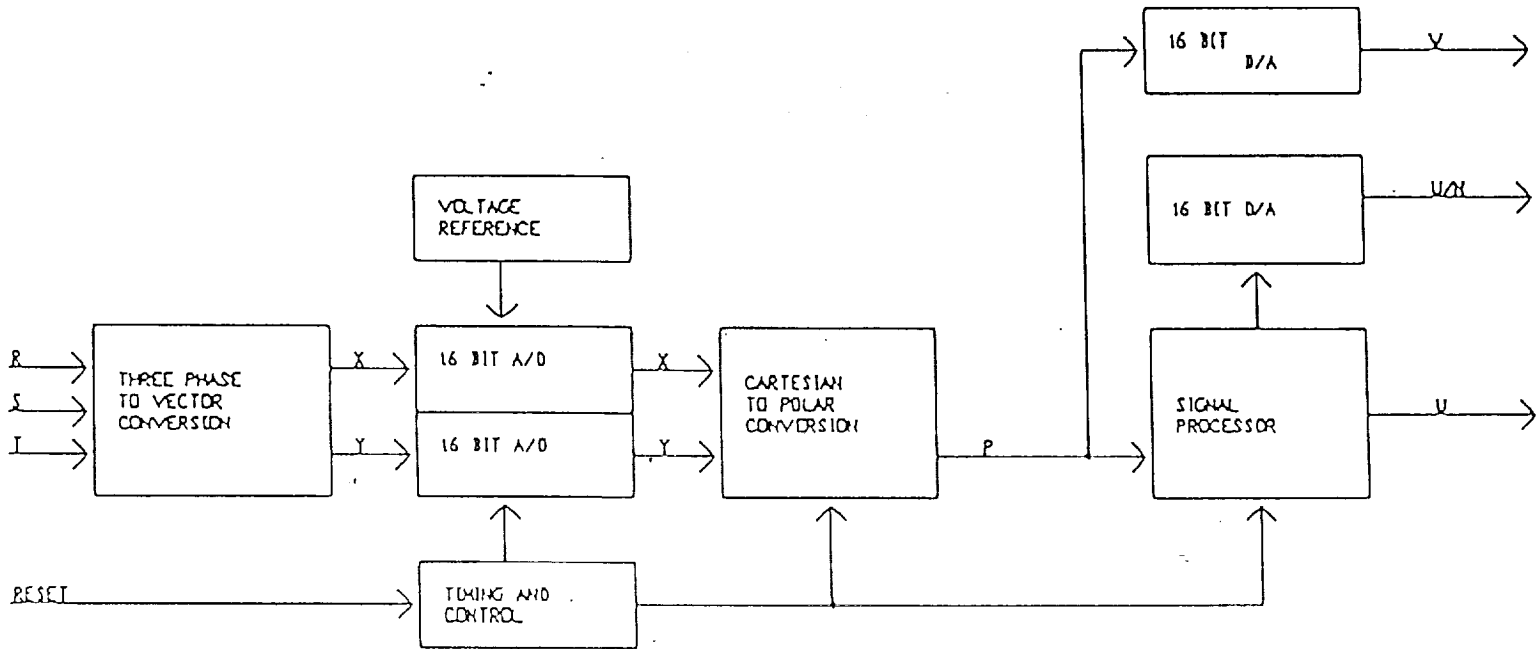
by a gradient index lens. It is followed by a quarter waveplate (QWP) and a birefringent calcite Wollaston prism (WP) which together form an analyzer. The WP has an angle of 1.9° and acts as a beamsplitter to give two beams, with different polarization states, determined by the orientation of the QWP. At the same time, it also produces a small difference in the angle the two beams (0.6°). This angular dispersion between the two components tilts their respective wavefronts and they cross interfering to form a fringe field of $75 \mu\text{m}$ spacing. This fringe spacing created by the WP is designed so the fringes will fall on a one dimensional array of 90 photodiodes, $25 \mu\text{m}$ in width. A polarizer at 45° is placed in front of the sensing elements to combine the two polarization states and allow interference to occur. The Wollaston prism, the polarizer and detector are all cemented into a single unit using a Norland index matching optical adhesive.

The one dimensional array of 90 photodiodes, has every third detector element tied together. By the inherent nature of an interference fringe pattern, the phase of the interference varies from 0 to $0+2\pi$ across each individual fringe. When the phase difference between the two beams changes (due to a current related magnetic field passing through the loop) the fringe pattern moves accordingly. With each detector being $25 \mu\text{m}$ wide and each fringe $75 \mu\text{m}$ wide, each detector covers $1/3$ of a cycle. Every third detector is tied together yielding three signals, R, S, and T, dependent on the intensity located within each fringe and hence its phase. It is this interferometric phase that carries the current information.

A block diagram of the signal processor is shown in Figure 7. The fundamental problem in interpreting interferometric phase measurements is to make precise determinations of the phase, ϕ , in the presence of unknown and varying light levels. The basic interferometric equation:

$$I(t) = I_1(t) + I_2(t) \cos[\phi(t)],$$

has the problem of three unknowns, I_1 , I_2 , and ϕ and only one equation.



FIBER OPTIC LOOP SIGNAL PROCESSING

Figure 7 Signal Processor Block Diagram

To get by this problem OPTRA has developed a technique called Multiphase Detection. It uses the three detector sets, R, S, and T with a spatial technique for introducing the differential phase shifts. The three detection signals are generated by:

$$\begin{aligned} R &= I_1 + I_2 \cos(\Phi_R); \Phi_R = \Phi \\ S &= I_1 + I_2 \cos(\Phi_S); \Phi_S = \Phi + 2\pi/3 \\ T &= I_1 + I_2 \cos(\Phi_T); \Phi_T = \Phi + 4\pi/3 \end{aligned}$$

These three phase signals are converted to vectors through the mathematical process:

$$\begin{aligned} X &= R - 0.5S - 0.5T \\ Y &= 0.886(S - T) \end{aligned}$$

These signals then pass through a AD1382, 16 Bit, 500 KHz, A/D converter to a TRW TMC2330 16 Bit coordinate transformation chip. This information is split and passed through: 1) a 16 Bit D/A converter yielding the wrapped signal proportional to the input phase, modulo 2π and 2) unwrapping electronics to generate a digital signal which replicates the input phase as a function of time.

The ideal phase resolution is given by

$$\begin{aligned} 1 \text{ fringe} / (2^{16} / 5 \times 10^5) &= 2.1 \times 10^{-8} \text{ fringe} / \sqrt{\text{Hz}} \\ &= 3 \times 10^{-7} \text{ radians} / \sqrt{\text{Hz}} \end{aligned}$$

The noise requirements to get 1 bit_{rms} accuracy at the phase output requires 0.7 bits_{rms} on each of the X and Y inputs. One least significant bit (1 LSB) is given by

$$1 \text{ LSB} = \pm V_{\text{input}} / 2^{16}$$

where $\pm V_{\text{input}}$ equals ± 10 volts yielding

$$1 \text{ LSB} = 3 \times 10^{-7} \text{ V} / \sqrt{\text{Hz}}$$

into the 16 bit A/D converters. As there is a gain of 2 and 1.5 in the R, S, T to X, Y conversion, the noise voltage, V_{noise} , equals

$$\begin{aligned} V_{\text{noise}} &= 215 \mu\text{V} / 2(1.5) = 7 \mu\text{V}_{\text{rms}} \\ &\text{or } 1 \times 10^{-7} \text{ V} / \sqrt{\text{Hz}} \end{aligned}$$

on R, S, and T.

The maximum sensitivity of the signal processing system can be no greater than the shot noise limit. An electric current is the flow of discrete electric charges. The finiteness of the charge

quantum results in statistical fluctuations of the current. If the charge acts independent of each other, the fluctuating current is given by:

$$I_{\text{shot noise}} = \sqrt{2qi}$$

where q is the electron charge (1.6×10^{-19} coulomb) and i is the photodiode current given by

$$i = V/R,$$

where V is the preamp output (10 volts) and R is the feedback resistance into the detector preamps (200 k Ω). Plugging the now given variables into the shot noise equation yields,

$$I_{\text{shot noise}} = 4 \times 10^{-12} \text{ amps}/\sqrt{\text{Hz}} \\ \text{or } 3 \times 10^{-7} \text{ rad}/\sqrt{\text{Hz}}.$$

Thus, the system has been designed so that the shot noise limit is equal to the minimum phase resolution of signal processing electronics.

4. SYSTEM PERFORMANCE

The optically isolated laser diode source module used in this experiment delivered 4.5 mW of linearly polarized light at the output of the HiBi fiber. The polarization extinction ratio is $\approx 1000:1$. The fiber optic loop of LoBi fiber was connected via a FC type connector. The output power from 1400 meters (total length) loop is 0.85 mW. After aligning the polarization at the interface of the HiBi and LoBi fiber, the extinction ratio at the output of the loop is $\approx 300:1$.

The fiber optic loop sensor performance is shown in Figure 8. It shows the expected theoretical results next to the actual measured results. Loop I is the configuration used in our experiment. Loop II is an extrapolation of Loop I results, using the entire length of fiber in one single turn loop. With a system noise of 6×10^{-7} rad/ $\sqrt{\text{Hz}}$, the minimum detectable current of our system was 5.4×10^{-5} amps/ $\text{m}^2/\sqrt{\text{Hz}}$. If space considerations were not an issue and we could use all of our 1400 meters of optical fiber in one turn, we could have achieved a minimum detectable current of 4×10^{-7} amps/ $\text{m}^2/\sqrt{\text{Hz}}$.

Figure 9 shows a photograph of data displayed on a spectrum analyzer. With 50 turns of wire wound around the fiber loop, 7.8 mA was driven through 50 copper turns. The loop sensed this as 0.39 amp turns. The spectrum analyzer trace of -55.1 dBV/ $\sqrt{\text{Hz}}$ corresponds to 5.4×10^{-4} rad/ $\sqrt{\text{Hz}}$ as the scale factor setting in the signal processor was set to 0.314 rad/volt. This compares favorably with the theoretical phase value of 5.5×10^{-4} rad/ $\sqrt{\text{Hz}}$

where phase, Φ , is given by:

$$\Phi = VJDL/2$$

- and
- V = Verdet coefficient of the fiber = 4.83×10^{-6}
 - J = current density = 0.4 amp turns/($8\text{m}^2 - \sqrt{300 \text{ MHz}}$)
 - D = diameter of fiber loop = 3.2 meters
 - L = total fiber length = 1400 meters

The sensor performance graph shows a minimum detectable phase of 6×10^{-7} rad/Hz. This is the system noise level. By dividing the signal phase by the minimum detectable phase a signal to noise ratio of 917:1 is obtained by,

$$S/N = \frac{\Phi_{\text{signal}}}{\Phi_{\text{min det}}} = \frac{917}{1}$$

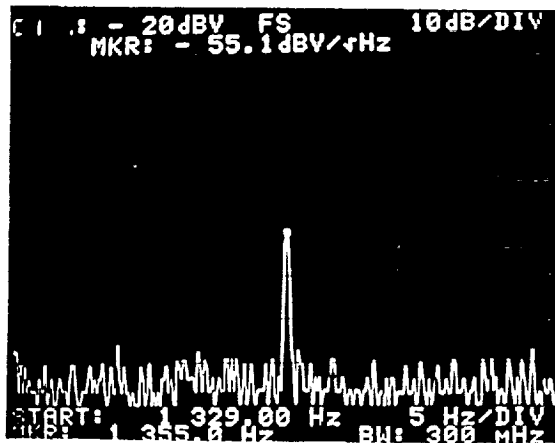
FIBER OPTIC LOOP RESULTS

| Loop I (L = 1400m, D = 3.2m, N = 137) | Theoretical | Measured |
|---------------------------------------|--|---|
| loop sensitivity | 0.011 radians/amp/m ² or 0.0018 fringes/amp/m ² | .012 radians/amp/m ² .0019 fringes/amp/m ² |
| minimum detectable phase | 3×10^{-7} radians/Hz or 4.8×10^{-8} fringes/Hz | 6×10^{-7} radians/Hz 9.6×10^{-8} fringes/Hz |
| minimum detectable current density | 2×10^{-5} amps/m ² /Hz | 5.4×10^{-5} amps/m ² /Hz |

| Loop II (L = 1400 m, D = 446 m, N = 1) | Projected |
|--|--|
| loop sensitivity | 1.5 radians/amp/m ² or .240 fringes/amp/m ² |
| minimum detectable phase | 6×10^{-7} radians/Hz* 9.6×10^{-8} fringes/Hz |
| minimum detectable current density | 4×10^{-7} amps/m ² /Hz |

* Measured minimum detectable phase for Loop I

Figure 8 System Performance



0.12 amp-turns applied
 @ 1330 Hz
 5.4×10^{-4} rad/√Hz

Figure 9 Phase Signal

Dividing the current density that corresponds to the signal phase by the S/N ratio, the minimum detectable current density, J , is determined by,

$$J_{\min} = \frac{J_{\text{sig}}}{\text{S/N}} = 5.4 \times 10^{-5} \frac{\text{amps}}{\text{m}^2/\text{Hz}}$$

Figure 10 shows the frequency response to be nearly flat from 150 Hz to 25 kHz. The limit of 25 kHz is limited only by the spectrum analyzer used in acquiring the data. The sensor linearity performance, shown in Figure 11, shows a nearly linear response over two orders of magnitude of phase from 2.5×10^{-3} to 4×10^{-5} radians.

A spectrum analyzer photograph of the system response to a 0.75 amp 150 Hz input, (Figure 12) shows a 1 mrad phase at 150 Hz and three 60 Hz noise components at 60 Hz, 120 Hz and 180 Hz. We believe this noise to originate at the laser diode current source and carried through the system via the laser light. If the loop is removed from the system this noise is still present. This indicates that the 60 Hz signals are not room fields being picked up by the loop. Several steps have been taken, including shielding the current source transformer, to reduce this to its present value.

The DC drift of the entire sensor system with and without loop is shown in Figures 13 and 14 respectively. The sensor system's

maximum DC drift over a 12 hour period is 35 mrad. From hour 2 to hour 12 there was a 5° Fahrenheit drop in ambient room temperature. The significance of Figure 14 (no loop), is that it shows the drift is not in the optical fiber loop but somewhere else. The signal processor's isolated DC drift is order of magnitude less than the entire system, the drift can be attributed to thermal drift in the optical adhesive used in our receiver optics. The phase, ϕ , in radians is related to movement between the optically adhered parts by the distance one fringe moves. As DC drift of 3.5×10^{-3} radians corresponds to a maximum thermal drift in the index matching epoxies of 3.8×10^{-6} meters.

FREQUENCY RESPONSE

Loop Sensitivity vs. Frequency

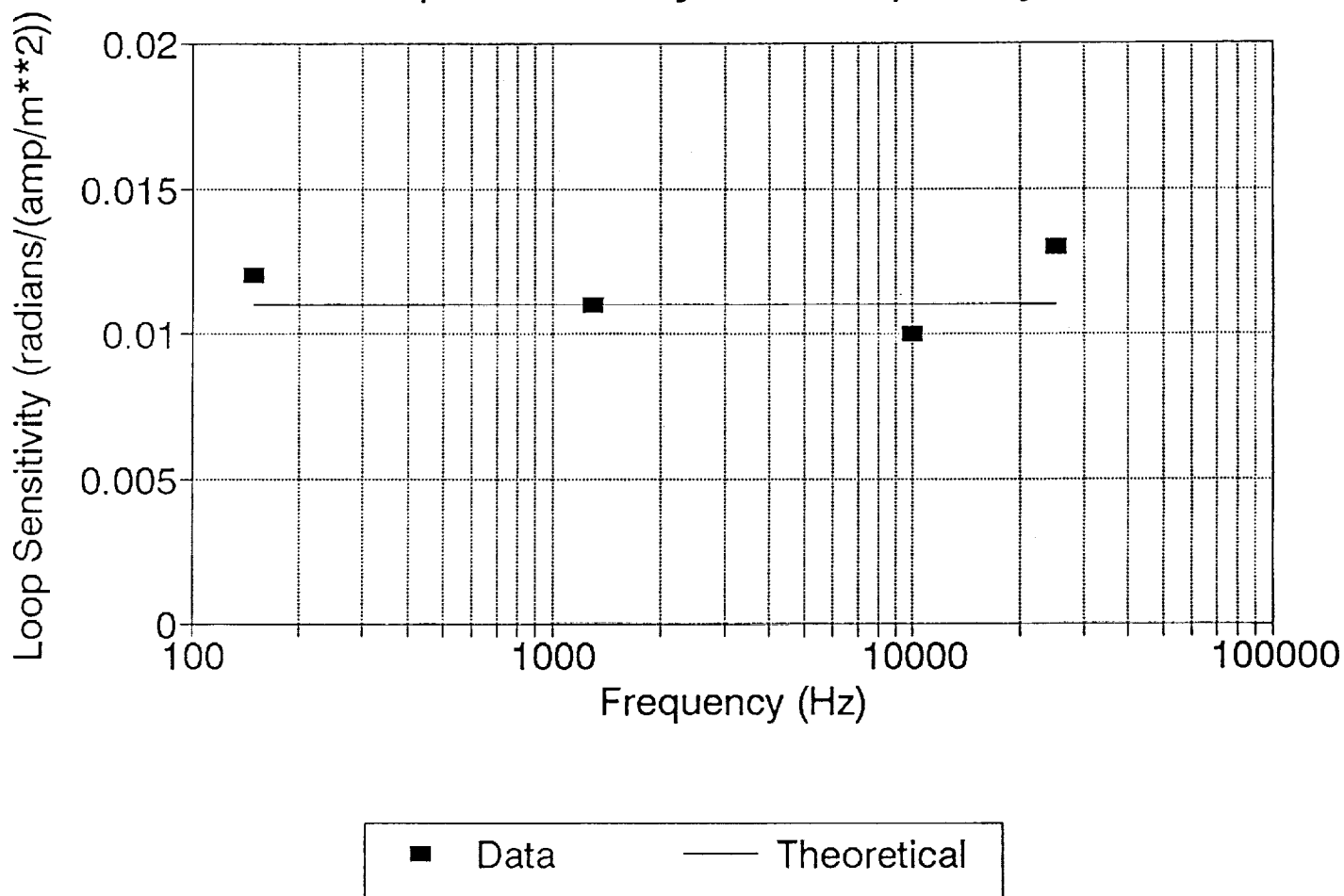


Figure 10

SENSOR LINEARITY

Phase vs. Current Density

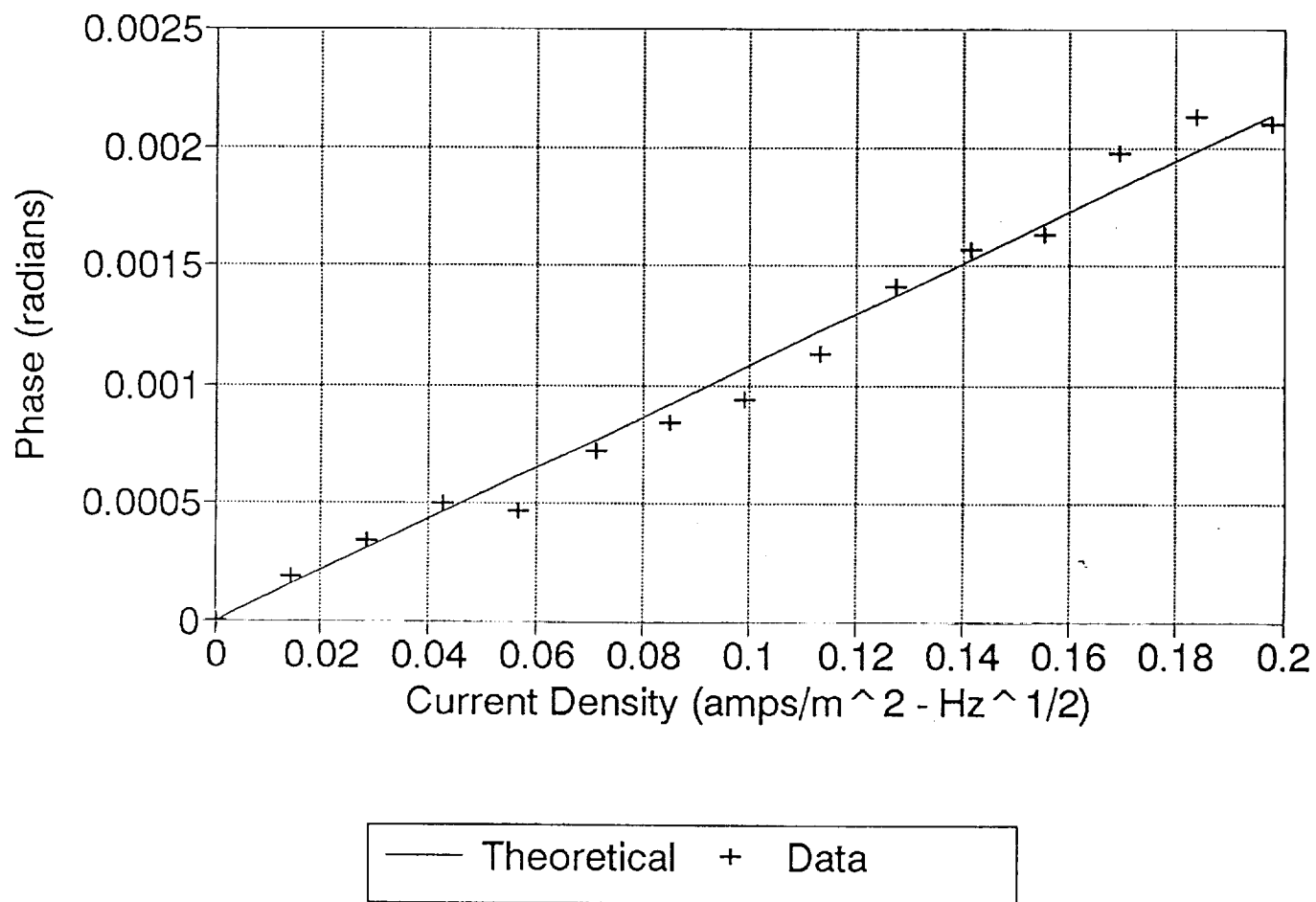
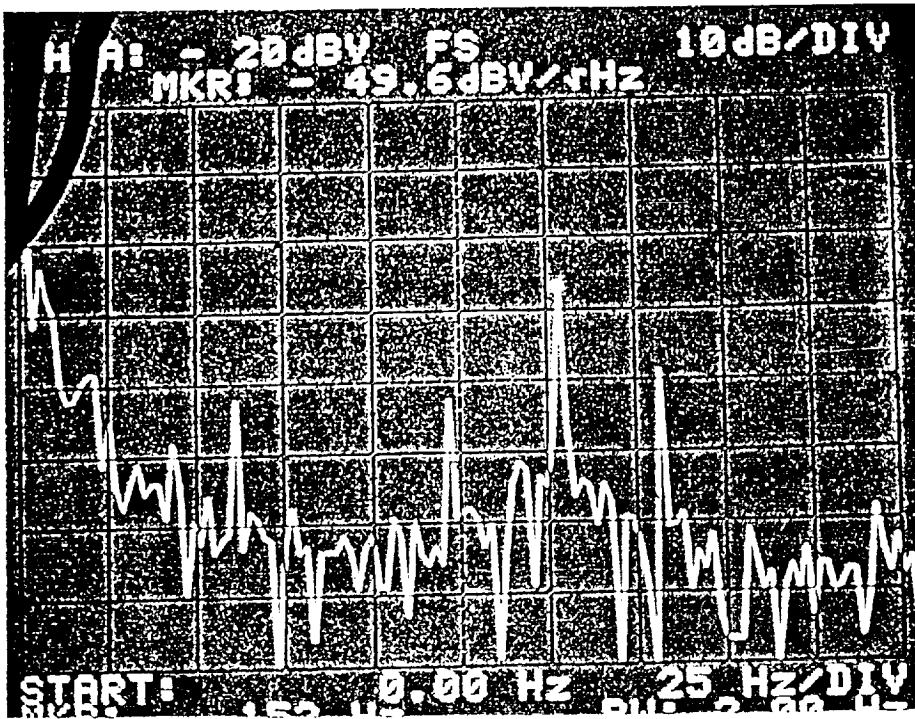


Figure 11



$1.0 \times 10^{-3} \text{ rad}/\sqrt{\text{Hz}}$

250 Hz

Figure 12 Frequency Response

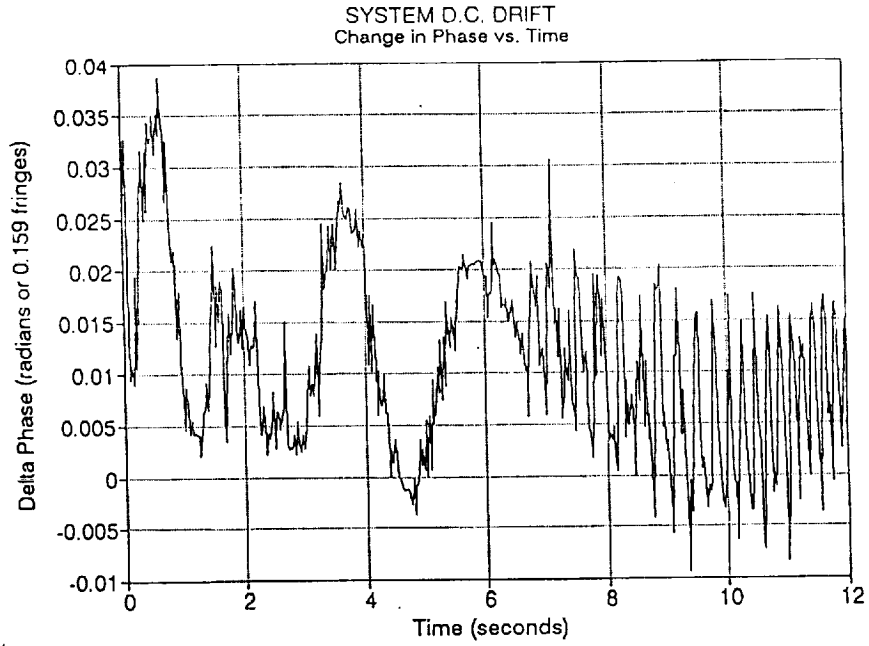


Figure 13

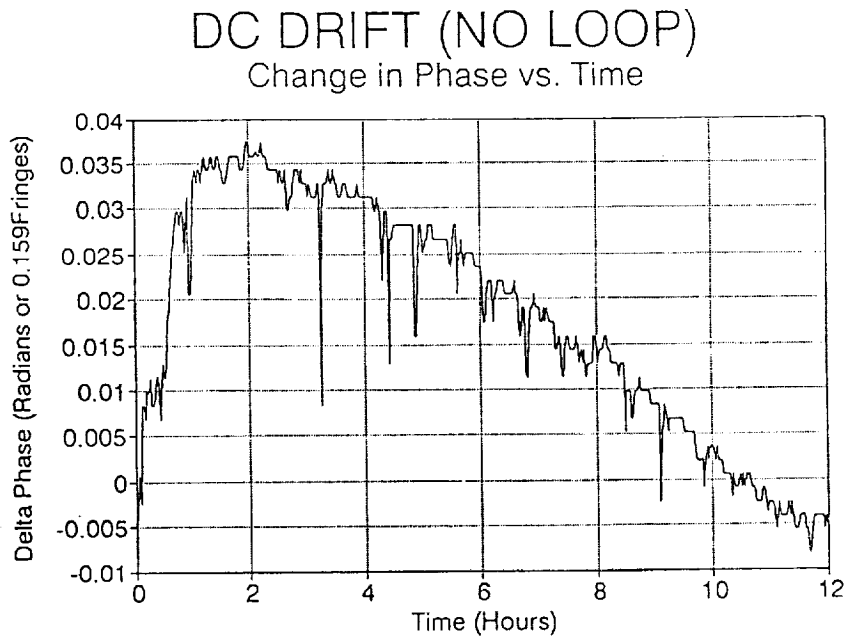


Figure 14

The result is that our receiver optics are being held to a tolerance of $0.38 \mu\text{m}$ or better. There are three interfaces that are possible sources of error. There is the interface in the Wollaston prism, the interface between the Wollaston and polarizer and the interface between polarizer and triphase detector.

The reason for selecting a Wollaston prism over a wedge, is that it automatically compensates for any path length mismatch in the interferometer. If a wedge is used, a compensation plate must also be used to correct for path mismatch. Figure 15 shows data taken to determine the change in phase due to the optical path difference (OPD) of our receiver optics. The slope of the trace in Figure 15 indicates the OPD, therefore,

$$\text{slope} = \Delta\phi/\Delta v$$

Therefore, the change in phase, $\Delta\phi$, due to any optical path mismatch in our interferometer is 3×10^{-8} radians.

OPTICAL PATH DIFFERENCE

Phase Difference vs. Current Change

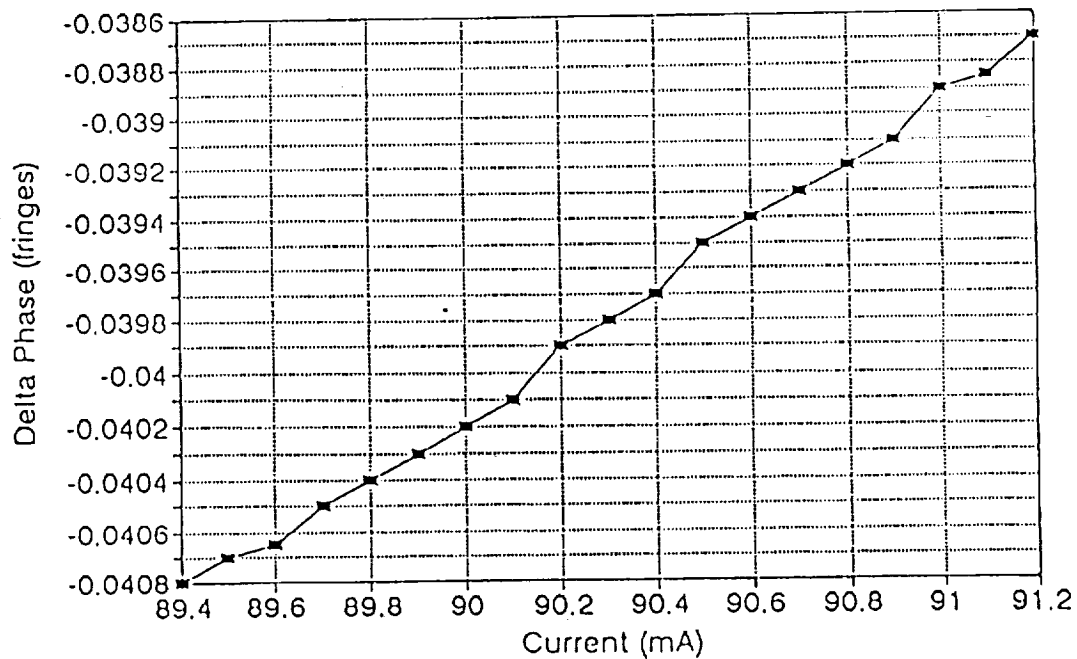


Figure 15

5. CONCLUSION

We have demonstrated experimentally that there is a great potential for a fiber optic loop sensor for the measurement of electrically charged particle fluxes in outer space. A prototype laser diode based fiber optic sensor was developed with a minimum detectable current density of 5.4×10^{-5} amps/m²/Hz. If laboratory space considerations were not an issue, we could have built a single turn loop with the 1400 meter fiber length available to us, and been able to achieve 4×10^{-7} amps/m²/Hz. The key advantage to this approach for measuring charged particles is the absence of any magnetic materials which might perturb the measurement of very small particle fluxes.

Potential applications for this prototype are clearly directed into the areas of the Space Program. Other areas that could potentially benefit from implementing this type of system are the measurement of displacement currents near power lines and the studying of lightning.

We believe the fiber optic loop sensor system worked extremely well. The signal processing electronics are capable of detecting phase shifts down to 6×10^{-7} radians/√Hz. The system is very linear over a wide range and has a bandwidth that exceeds 25 kHz. The only deficiency was in the area of DC measurements. Although the thermal stability of the receiver optics holds to better than $0.4 \mu\text{m}$, to achieve a target minimum detectable current density of $1 \mu\text{amp}/\text{m}^2/\text{Hz}$ a stability on the order of 2.6×10^{-13} m is required. Our major recommendation for the deployment of this sensor system is to either enclose the receiver optics in a isothermal housing or attach a thermistor to it and thermo-electrically temperature control it.

APPENDIX A

Also performed under this program was temperature testing and DC field testing. The temperature performance evaluation of the fiber optic loop sensor is discussed in Section 4 along with DC drift.

DC field testing was performed in two separate tests. The two tests consisted of a DC current being driven through the loop and a magnetic field being passed through the loop. The resulting phase shift from an 11.25 amp DC/m² current being sent through the loop is shown in Figure A1. The associated drift in the oscilloscope trace corresponds to the DC drift rate described in Section 4. The system works well in detecting DC currents, but the DC drift rate dictates that the minimum DC current induced phase shift be above the 35 mrad phase drift.

When a 200 gauss magnetic field was passed through the loop there was no result detected (see Figure A2). As current and not magnetic field is detected by this sensor system, this was the anticipated result. As the earth's magnetic field is 0.5 gauss, this test shows more than sufficient isolation from external magnetic fields.

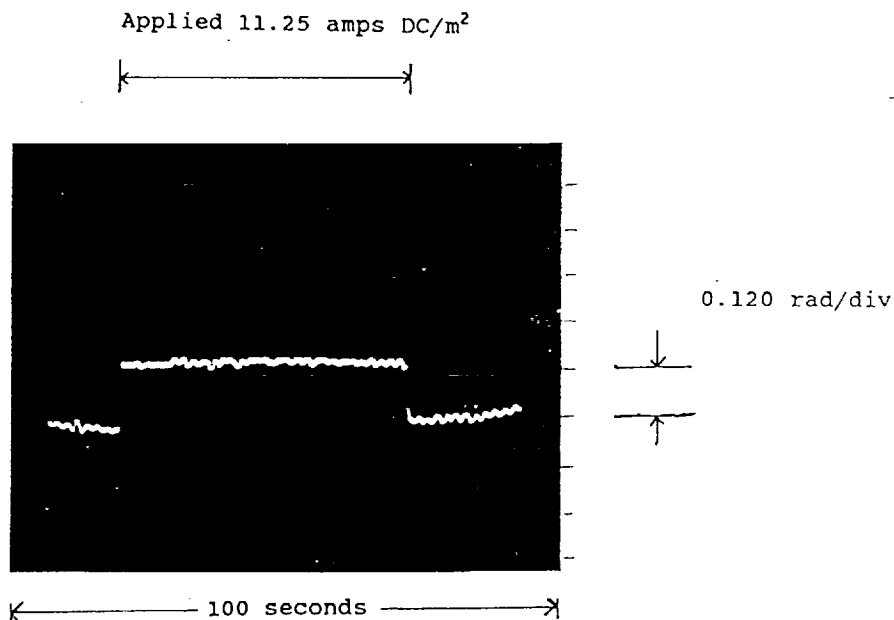


Figure A1 Applied DC Current

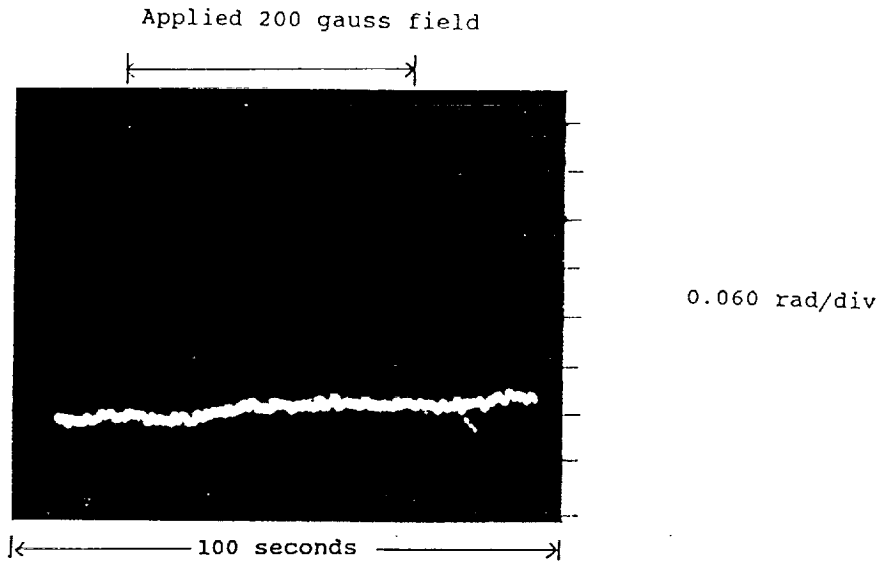


Figure A2 Applied Magnetic Field